


# Cytotoxic and genotoxic evaluation of different synthetic amorphous silica nanomaterials in the V79 cell line

Toxicology and Industrial Health  
1–12  
© The Author(s) 2015  
Reprints and permissions:  
sagepub.co.uk/journalsPermissions.nav  
DOI: 10.1177/0748233715572562  
tih.sagepub.com  


Y Guichard, C Fontana, E Chavinier, F Terzetti, L Gaté,  
S Binet and C Darne

## Abstract

The nature of occupational risks and hazards in industries that produce or use synthetic amorphous silica (SAS) nanoparticles is still under discussion. Manufactured SAS occur in amorphous form and can be divided into two main types according to the production process, namely, pyrogenic silica (powder) and precipitated silica (powder, gel or colloid). The physical and chemical properties of SAS may vary in terms of particle size, surface area, agglomeration state or purity, and differences in their toxicity potential might therefore be expected. The aim of this study was to compare the cytotoxicity and genotoxicity of representative manufactured SAS samples in Chinese hamster lung fibroblasts (V79 cells). Five samples from industrial SAS producers were evaluated, that is, two pyrogenic SAS powders (with primary particle sizes of 20 nm and 25/70 nm), one precipitated SAS powder (20 nm) and two precipitated SAS colloids (15 and 40/80 nm). V79 cell cultures were treated with different concentrations of SAS pre-dispersed in bovine serum albumin–water medium. Pyr (pyrogenic) 20, Pre (precipitated) 20 and Col (colloid) 15 significantly decreased the cell viability after 24 h of exposure, whilst Pyr 25/70 and Col 40/80 had negligible effects. The cytotoxicity of Pyr 20, Pre 20 and Col 15 was revealed by the induction of apoptosis, and Pyr 20 and Col 15 also produced DNA damage. However, none of the SAS samples generated intracellular reactive oxidative species, micronuclei or genomic mutations in V79 cells after 24 h of exposure. Overall, the results of this study show that pyrogenic, precipitated and colloidal manufactured SAS of around 20 nm primary particle size can produce significant cytotoxic and genotoxic effects in V79 cells. In contrast, the coarser-grained pyrogenic and colloid SAS (approximately 50 nm) yielded negligible toxicity, despite having been manufactured by same processes as their finer-grained equivalents. To explain these differences, the influence of particle agglomeration and oxidative species formation is discussed.

## Keywords

Synthetic amorphous silica, V79 cell line, cytotoxicity, micronucleus, comet assay, HPRT assay

## Introduction

Synthetic amorphous silica (SAS) products were first commercialized in the 1950s. By 2006, worldwide production was estimated to be one million tons per year (ECETOC, 2006). SAS correspond to the definition of nanomaterials agreed by the European Community (EC, 2011). They are used in a wide variety of industrial applications, including as reinforcement and thickening agents in elastomers, resins and inks. Applications in consumer products include cosmetics, pharmaceuticals and as direct food and feed additives. SAS can be divided into two groups according to

whether the manufacturing process is via the wet route (precipitated silica, silica gel and colloidal silica) or the thermal route (pyrogenic silica). In brief, precipitated, gel and colloidal silica products (CAS

---

Institut National de Recherche et de Sécurité (INRS), Vandoeuvre Cedex, France

### Corresponding author:

Y Guichard, Institut National de Recherche et de Sécurité, rue du Morvan, CS 60027, 54519 Vandoeuvre Cedex, France.  
Email: yves.guichard@inrs.fr

112926-00-8) are obtained by acidification of sodium silicate under wet conditions. The resulting gelatinous precipitate is then transformed into either precipitated silica nanoparticles (powder) or silica gel, depending on the washing, ageing, drying and milling conditions. Partial neutralization of alkali silicate solution followed by ion exchange produces colloidal silica consisting of particle suspensions in water. Pyrogenic silica (CAS 112945-52-5) is produced by hydrolysis of silicon tetrachloride at high temperature ( $>1000^{\circ}\text{C}$ ) (Fruijtier-Polloth, 2012). Unlike crystalline silica, which has been classified as carcinogenic to humans (group 1) by the International Agency for Research of Cancer (IARC), SAS has not been classifiable as to its carcinogenicity to humans (group 3) (IARC, 1997). However, concerns remain regarding the hazards and risks of SAS nanomaterials for producers and users. Whilst several *in vitro* and *in vivo* studies have reported cytotoxic and inflammatory effects induced by manufactured or laboratory-synthesized SAS (Fruijtier-Polloth, 2012; Napierska et al., 2010), data on the genotoxicity of manufactured SAS (excluding those synthesized in the laboratory for research purposes) are more limited. In an *in vivo* study, no increase in mutation in the hypoxanthine guanine phosphoribosyltransferase (HPRT) gene was found in alveolar epithelial cells from rats exposed by inhalation to Aerosil 200<sup>®</sup>, a pyrogenic SAS, for 13 weeks at  $50\text{ mg m}^{-3}$  (Johnston et al., 2000). In another study, slight DNA damage, assessed in liver by the comet assay, and weak induction of micronucleated reticulocytes were detected in rats treated with repeated injection of the colloidal SAS Levasil 200<sup>®</sup> (15 nm primary particle size) and Levasil 50<sup>®</sup> (55 nm) at  $50\text{ mg kg}^{-1}$ . However, the micronucleus assay in human blood lymphocytes exposed to these colloids was negative (Downs et al., 2012). *In vitro*, comet assays performed with different colloidal SAS from Glantreo (33, 34 and 240 nm) and Sigma-Aldrich (21 and 30 nm) were all negative in 3T3-L1 fibroblasts treated with SAS at concentrations of 4 and  $40\text{ }\mu\text{g mL}^{-1}$  for 3, 6 and 24 h (Barnes et al., 2008), respectively. In contrast, comet assays performed in HT29, HaCat and A549 cell lines exposed to colloidal Ludox SM-30<sup>®</sup> (14 nm) at 0.1, 1 and  $10\text{ }\mu\text{g mL}^{-1}$  for 24 h showed an increase in DNA damage with a dose–response relationship for all cell lines (Mu et al., 2012). A pyrogenic SAS from Sigma-Aldrich (14 nm) responded positively in comet assays performed in the Caco-2 cell line following 4 h treatment with SAS at  $20\text{ }\mu\text{g cm}^{-2}$  (Gerloff et al., 2009).

More recently, two precipitated SAS powders (12 and 14 nm) and two pyrogenic SAS powders (10 and 16 nm) were found to be incapable of inducing micronuclei in human lymphocyte exposed to up to  $1250\text{ }\mu\text{g mL}^{-1}$  of SAS over 24 h (Tavares et al., 2014). Together, the literature data suggest that the genotoxicity of manufactured SAS may depend on the procedures used to synthesize them, which in turn determine their different physical and chemical properties (e.g. primary size, surface area, aggregation/agglomeration state and degree of purity). Cytotoxic and genotoxic cellular response to SAS is probably also associated with the cell type, the method of SAS dispersion (medium and mode of agitation) and the composition of the cell culture medium (e.g. the serum concentration). The aim of this study was to evaluate in the same *in vitro* model (the V79 cell line) the genotoxicity of samples representative of manufactured pyrogenic and precipitated SAS (powders and colloids). Genotoxicity was assessed by the micronucleus assay, the formamidopyrimidine DNA glycosylase (FPG)-modified comet assay and the HPRT gene mutation assay. Cell viability, apoptosis and reactive oxidative species (ROS) assays were also carried out for a comprehensive assessment of the genotoxic effects induced by SAS in V79 cells.

## Materials and methods

### Physicochemical characterization of SAS

All samples (two pyrogenic samples of different particle sizes, one precipitated sample and two colloid samples of different sizes) were kindly provided by industrial producers. Primary particle-size distribution was determined by transmission electronic microscopy (TEM) with an EM910 100kV (Zeiss, Germany) (Figure 1). For the purpose of this study, the SAS samples were assigned names that denote the manufacturing process used ('Pyr' for pyrogenic, 'Pre' for precipitated and 'Col' for colloid) and an approximation of their primary size in nanometres (Pyr 20, Pyr 25/70, Pre 20, Col 15 and Col 40/80) (Table 1). The specific surface area (SSA) of sample powders was determined by nitrogen gas adsorption with a BELSORP-Max (BEL Japan, Inc., Japan) using the Brunauer, Emmett and Teller (BET) calculation method (Brunauer et al., 1938). For impurity analysis, concentrations of major elements (sodium, magnesium, aluminium, potassium, calcium, titanium, manganese, iron, barium, copper and zinc) were determined by inductively coupled plasma and

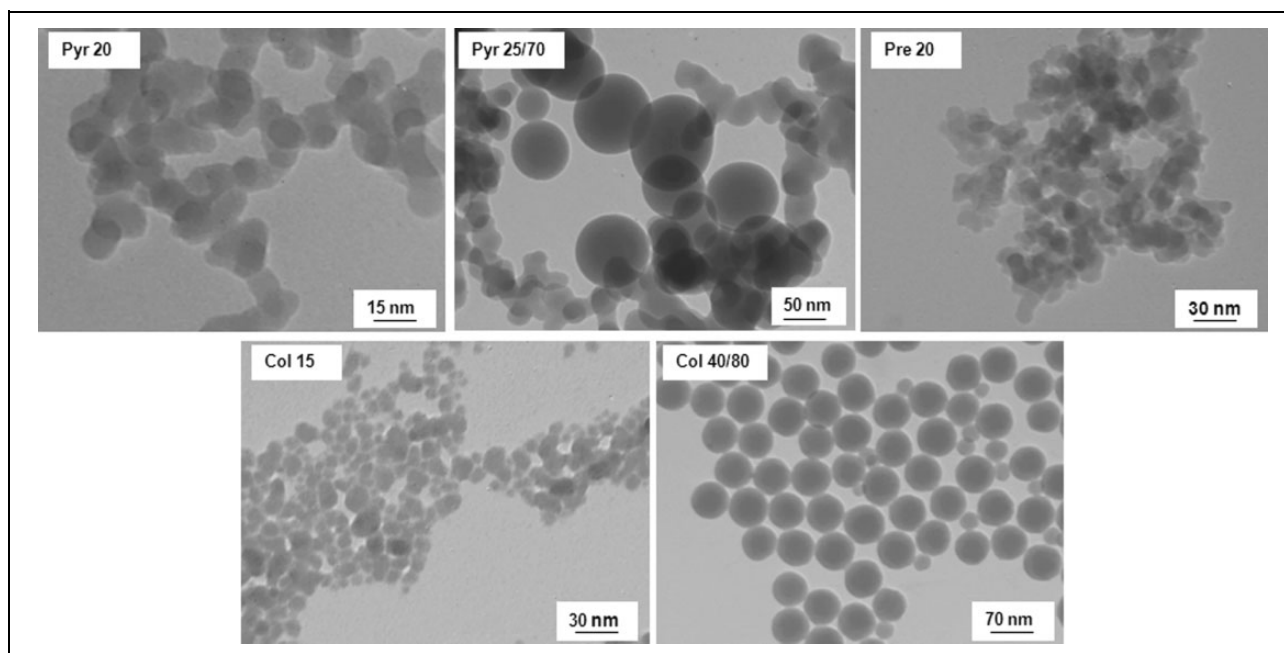


**Figure 1.** TEM images of the different SAS used in this study. TEM: transmission electronic microscopy; SAS: synthetic amorphous silica.

**Table 1.** Chemical and physical particle characteristics.

SAS	Impurity <sup>a</sup>	SSA (m <sup>2</sup> g <sup>-1</sup> ) <sup>b</sup>	Primary size (nm) <sup>c</sup>	Size in BSA–water (nm) <sup>d</sup>	Size in culture medium (nm) <sup>d</sup>
Pyr 20	<0.5%	184	19 ± 5	176 ± 3	250 ± 7
Pyr 25/70	<0.5%	42	71 ± 25 (≈50%) 25 ± 8 (≈50%)	196 ± 1	281 ± 9
Pre 20	1% Na	207	19 ± 3	n.d	n.d
Col 15	0.8% Na	≈200 <sup>e</sup>	15 ± 4	35 ± 0.4	174 ± 4
Col 40/80	<0.5%	≈50 <sup>e</sup>	79 ± 3 (≈80%) 38 ± 5 (≈20%)	87 ± 1	117 ± 2

n.d: not determined; SAS: synthetic amorphous silica; BSA: bovine serum albumin; SSA: specific surface area; ICP-AES: inductively coupled plasma and atomic emission spectrometry; ICP-MS: inductively coupled plasma and mass spectrometry; BET: Brunauer, Emmett and Teller; TEM: transmission electronic microscopy; DLS: dynamic light scattering.

<sup>a</sup>ICP-AES and ICP-MS analyses (percentage of mass).

<sup>b</sup>BET analysis.

<sup>c</sup>TEM analysis (mean diameter ± SD of 100 measurements).

<sup>d</sup>DLS analysis (mean hydrodynamic diameter ± SD of three assays).

<sup>e</sup>Calculated from the primary size.

atomic emission spectrometry (ICP-AES), and concentrations of trace elements (chromium, cobalt, vanadium, nickel, arsenic, cadmium and lead) by ICP mass spectrometry (ICP-MS) using an 820-MS (Varian, Australia). The hydrodynamic size of particles, pre-diluted in the dispersion medium and then diluted in the cell culture medium (see ‘Preparation of SAS and cell treatment’ section), was determined for the highest concentration used in *in vitro* assays by dynamic light scattering (DLS) using a Zetasizer Nano ZS (Malvern Inc., UK).

### Cell culture

The V79 cell line (lung fibroblast from Chinese hamster, reference CCL-93, ATCC, Manassas, Virginia, USA) was selected for this study as it is one of the cell models recommended in OCDE guidelines 487 and 476 for use in the *in vitro* micronucleus assay and in the *in vitro* HPRT assay, respectively. Cells were grown in Dulbecco’s modified Eagle’s medium (Invitrogen, France), supplemented with 10% foetal calf serum (FCS, PAN Biotech, France) and antibiotics

(50 U mL<sup>-1</sup> penicillin, 50 µg mL<sup>-1</sup> streptomycin, Invitrogen). Cells were incubated at 37°C and 5% carbon dioxide. Under these conditions, the doubling time of V79 cells was approximately 14 h.

### Preparation of SAS and cell treatment

SAS suspensions for cell treatment were prepared according to the procedure described by Jensen et al. (2011). A 5.25 mg mL<sup>-1</sup> dispersion of SAS powders was prepared by pre-wetting the powders in 0.5 vol% ethanol followed by addition of sterile-filtered 0.05 wt% bovine serum albumin (BSA, Sigma-Aldrich) water. Next, the SAS suspension underwent ultrasonication for 16 min on ice using a Branson sonifier 450 (Branson Ultrasonics Corp, Danbury, Connecticut, USA) set at 10% amplitude. The two colloidal samples Col 15 and Col 40/80, which were purchased at initial concentrations of 381 and 369 mg mL<sup>-1</sup>, respectively, were not sonicated. Serial dilutions of all SAS were prepared in 0.05 wt% BSA–water (0.655, 1.31, 2.62 and 5.25 mg mL<sup>-1</sup>). An aliquot of each of these preparations was immediately diluted 10 times in the cell culture medium, leading to final SAS concentrations of 66, 131, 262 and 525 µg mL<sup>-1</sup>. In this study, SAS concentrations are expressed as mass per cell culture surface area and correspond to concentrations of 12.5, 25, 50 and 100 µg cm<sup>-2</sup>.

### Viability assay

Cell viability was measured using the cell proliferation reagent WST-1 (Roche Diagnostics, France). The method is based on the cleavage of WST-1 tetrazolium salt by mitochondrial dehydrogenases in viable cells to a water-soluble formazan dye. First, 1 × 10<sup>4</sup> cells in 100 µL of culture medium were seeded in a 96-well culture plate (0.32 cm<sup>2</sup> per well) and incubated for 24 h prior to treatment. The cells were then treated for 24 h with 10 µL of either BSA–water alone (control) or BSA–water containing SAS dilutions. In parallel, a 96-well culture plate received culture medium that contained no cells but the same treatment dilution in order to assess potential interference between the SAS and the WST-1 reagent. After treatment, 1/10 (v/v) WST-1 reagent was added to each well and incubated for 3 h. Plates were then centrifuged at 4500 r min<sup>-1</sup> for 5 min. Supernatants were transferred to new 96-well plates and optical density (OD) was recorded at 450 and 690 nm using a microtiter plate reader (Synergy HT, BioTek, France). The

delta OD (OD<sub>450 nm</sub> – OD<sub>690 nm</sub>) was then calculated. Cell viability was expressed by the percentage of the delta OD in treated cells with respect to the control.

### Caspase-3 assay

The EnzChek<sup>®</sup> Caspase-3 Assay Kit #2 (Molecular Probe, Invitrogen) was used for the detection of apoptosis. This assay measures the protease activity of caspase-3 with the aspartic acid (Asp)–glutamic acid–valine–Asp (DEVD) amino acid sequence. The substrate used in the assay is a rhodamine 110 derivative covalently linked to DEVD peptides, thereby suppressing the dye fluorescence. Upon enzymatic cleavage by caspase-3, the non-fluorescent substrate is converted to a fluorescent rhodamine 110 derivative. Twenty-four hours prior to treatment, 4 × 10<sup>5</sup> cells in 4 mL of culture medium were seeded in 60-mm culture dishes (21 cm<sup>2</sup>) and then treated for 24 h with 400 µL of BSA–water either alone (for the control) or containing SAS dilutions. At the end of treatment, cells were washed in Hank's balanced salt solution (Invitrogen) and harvested using 0.25% trypsin (Invitrogen). Cell cultures that had been deprived of FCS for 18 h were used as a positive control for apoptosis induction in V79, as described in a previous study (Hasan et al., 1999). At the end of treatment, an aliquot of 1 × 10<sup>6</sup> cells was washed in PBS and suspended in 50 µL of cell lysis buffer (contained in the Kit #2) on ice for 30 min. The mixture was then centrifuged at 6000 r min<sup>-1</sup> for 5 min. Fifty microlitres of the supernatant were transferred in a 96-well plate and 50 µL of substrate solution (containing rhodamine 110-DEVD peptides) was added and samples were incubated at room temperature for 30 min. Fluorescence was recorded using a microtiter plate reader (Synergy HT, BioTek) with excitation at 485 nm and emission detection at 530 nm. An aldehyde Ac-DEVD-CHO inhibitor was used to confirm that the observed fluorescence signal was due to the activity of caspase-3. Next, 1 µL of Ac-DEVD-CHO inhibitor solution was added to selected samples that were then incubated at room temperature for 10 min before adding the substrate solution. In all cases, the increase in caspase-3 activity was expressed by the fold change in the measured fluorescence intensity of treated cells with respect to the control.

### FPG-modified comet assay

DNA damage was assessed by performing both versions of the alkaline comet assay, that is, with and

without the use of the FPG. The glycosylase FPG enzyme recognizes and cuts modified DNA bases, such as oxidative bases (e.g. 8-oxoguanine) (Tice et al., 2000) and alkylated bases (Speit et al., 2004). Base cleavages produce apurinic sites that are converted into strand breaks by the associated apurinic/aprimidinic-endonuclease activity of FPG. We followed the procedure of Collins et al. (1998), with some minor modifications. Cells were grown, treated for either 3 or 24 h and then harvested under the same conditions used for the caspase-3 assay. Cultures treated with 125  $\mu\text{M}$  methyl methanesulphonate (MMS, Sigma-Aldrich) were used as a positive control according to Speit et al. (2004). At the end of treatment, the recovered cells were embedded in 1% low-melting agarose (Sigma-Aldrich). Aliquots of the cell-agarose mixtures were then loaded onto slides pre-coated with 1% normal melting agarose (Sigma-Aldrich). Slides were immersed in cold lysis solution (2.5 M sodium chloride, 100 mM dihydrate ethylenediaminetetraacetic acid ( $\text{Na}_2\text{EDTA}$ ), 10 mM tris(hydroxymethyl)aminomethane-hydrochloric acid (Tris-HCl) with 1% Triton X-100 and 10% dimethyl sulphoxide) for 1 h at 4°C. Slides were then drained and pre-incubated in the FPG incubation buffer (Hepes 40 mM, potassium chloride 0.1 M, EDTA 0.5 mM, and BSA 0.2 mg  $\text{mL}^{-1}$ ; pH 8) for 15 min at 4°C. After draining, slides were incubated for 30 min at 37°C in fresh FPG incubation buffer containing either 5  $\text{U mL}^{-1}$  of FPG (Sigma-Aldrich) or no FPG. Slides were then drained and immersed in cold alkaline solution (300 mM sodium hydroxide and 1 mM  $\text{Na}_2\text{EDTA}$ ; pH 13) for 20 min. Electrophoresis was performed in the same buffer at 0.7 V  $\text{cm}^{-1}$  for 40 min. The slides were then washed with 0.4 M Tris-HCl for 15 min, and DNA was then stained with propidium iodide (2.5  $\mu\text{g mL}^{-1}$ ) for 1 h. Comet analysis was performed using a fluorescence microscope equipped with image analyzer software (Comet Assay IV, Perceptive Instruments, UK). The extent of DNA damage was determined on the basis of the median tail DNA from 100 cells.

### *Intracellular ROS assay*

Intracellular ROS was detected with the 5-(and-6)-chloromethyl-2',7'-dichlorodihydrofluorescein diacetate fluorescence probe (CM-DCFDA, Molecular Probe, Invitrogen). DCFDA derivatives detect a variety of ROS, including hydrogen peroxide, peroxy radicals and peroxynitrite anions (LeBel et al., 1992). As in the cell viability assay, cells were grown and treated with

SAS in a 96-well plate. Following the protocol described by Guichard et al. (2012), a sample of nano-size anatase titanium dioxide ( $\text{TiO}_2$ ) was used as a positive control. At the end of treatment, the wells were washed with PBS and 50  $\mu\text{L}$  of CM-DCFDA was added to give a final concentration of 5  $\mu\text{M}$ . The plate was then incubated at 37°C for 30 min. Wells were then washed with PBS and the fluorescence was recorded using a microtiter plate reader (Synergy HT, BioTek) with excitation at 485 nm and emission detection at 530 nm. ROS induction was expressed by the fold change in the measured fluorescence intensity of treated cells with respect to the control.

### *Micronucleus assay*

In 800  $\mu\text{L}$  of culture medium,  $1 \times 10^5$  cells were seeded in Labtek<sup>®</sup> slides (Nunc A/S, Denmark; 4  $\text{cm}^2$ ) 24 h prior to treatment and then treated for 24 h with 80  $\mu\text{L}$  of BSA-water, alone for the control, or containing SAS dilutions, or containing 125  $\mu\text{M}$  MMS (final concentration) as a positive control (Lasne et al., 1984). At the end of treatment, slides were washed with PBS, fixed in methanol for 15 min and left to dry at room temperature. DNA was stained with Pro Long Gold antifade reagent<sup>®</sup> with DAPI (Molecular Probe, Invitrogen). Micronuclei frequency was determined by scoring the number of micronucleated cells (containing at least one micronucleus) in 1000 cells per slide. Apoptotic cells were scored at the same time. The presence of SAS agglomerates on the slides did not interfere with the readings.

### *HPRT assays*

Mutation induction was assessed at the HPRT locus in V79 cells by 6-thioguanine selection, as described by the OECD 476 guideline. In 10 mL of culture medium,  $1 \times 10^6$  cells were seeded in 100-mm culture dishes (55  $\text{cm}^2$ ) 24 h prior to treatment. The cells were then treated for 24 h with 1 mL of culture medium (medium alone for the control, medium containing SAS dilutions or medium containing ethyl methanesulphonate (EMS), Sigma-Aldrich, at 400  $\mu\text{M}$  as a positive control according to the OECD 476 guideline). Cells were harvested at the end of treatment and aliquots of  $1 \times 10^5$  cells were grown for 6 days in new plates, during which time the cells were passaged once. Cells were then harvested and seeded in ten 100-mm culture dishes ( $2 \times 10^5$  cells/dish) in the presence of 6-thioguanine (6-TG, 5  $\mu\text{g mL}^{-1}$ , Sigma-Aldrich) and in ten 60-mm culture dishes

(100 cells/dish) in the absence of 6-TG. Cultures without 6-TG were grown over 7 days and those with 6-TG were grown over 10 days. The cell cultures were then washed in PBS, fixed in ethanol for 15 min, stained with 10% Giemsa (Merk, Germany) for 15 min and then scored. The percentage of surviving cells (the cloning efficiency) was determined by dividing the number of colonies scored by the number of cells seeded without 6-TG. HPRT mutant frequency per  $10^6$  surviving cells was calculated using the cloning efficiency and the number of cells seeded for mutation selection with 6-TG.

### Statistics

All experiments were carried out on at least three biological replicates. Data were analysed by one-way analysis of variance using the Statgraphics Centurion software (Statpoint Technologies, Warrenton, Virginia, USA). Fisher's least significant difference test was used to determine significance relative to the control and  $p < 0.05$  was considered significant.

## Results

### SAS sample characterization

The physicochemical characteristics of the SAS used in this study are described in Table 1. Chemical impurities were determined by ICP-AES and ICP-MS and were found to constitute less than 1% of total mass for all samples. TEM analysis showed that samples Pyr 20, Pre 20 and Col 15 were of similar primary particle size (around 20 nm), and particle size was relatively homogeneous in each of these samples. In contrast, samples Pyr 25/70 and Col 40/80 were composed of bimodal particle-size populations (25 and 70 nm in Pyr 25/70 and 40 and 80 nm in Col 40/80). As expected, the SSA values of the finer-grained SAS (Pyr 20, Pre 20 and Col 15) were much higher than those of the coarser-grained SAS (Pyr 25/70 and Col 40/80). As the BET method could not be used for the colloid samples, the SSA of Col 15 and Col 40/80 was calculated from their primary sizes. Particle sizes of samples in liquid phase were analysed by the DLS method at the highest SAS concentrations used in *in vitro* assays. DLS assays were performed both with SAS pre-dispersed in the BSA–water mixture (at  $5.25 \text{ mg mL}^{-1}$ ) and with the corresponding dilution in the culture medium (final concentration of  $525 \text{ }\mu\text{g mL}^{-1}$ ). DLS analysis of SAS pre-diluted in BSA–water showed that all SAS formed mono-dispersed

agglomerates of nanometric and submicrometric size (from 35 nm to 176 nm, depending on the SAS). SAS agglomerates were larger when diluted in the culture medium than when in BSA–water, and can be ranked as follows: Pyr 25/70 ( $\approx 280 \text{ nm}$ ) > Pyr 20 ( $\approx 250 \text{ nm}$ ) > Col 15 ( $\approx 170 \text{ nm}$ ) > Col 40/80 ( $\approx 120 \text{ nm}$ ). DLS measurements could not be performed on Pre 20 in BSA–water or in culture medium because the particle-size distribution was outside the range of detection of the system. Microscopic observation of Pre 20 in BSA–water or diluted in the culture medium revealed the presence of large micron-scale agglomerates (up to  $10 \text{ }\mu\text{M}$  in size) that cannot be analysed by DLS.

### Cell viability

Results showed that the finer SAS samples (Pyr 20, Pre 20 and Col 15) were more cytotoxic in V79 cells than the coarser samples Pyr 25/70 and Col 40/80 (Figure 2). The two coarse samples had negligible cytotoxic effect even at a relatively high concentration of  $100 \text{ }\mu\text{g cm}^{-2}$ . Col 15 was the most cytotoxic sample ( $53 \pm 1\%$  of cell viability at  $100 \text{ }\mu\text{g cm}^{-2}$ ). Considering the level of cytotoxicity for Col 15, we did not test concentrations higher than  $100 \text{ }\mu\text{g cm}^{-2}$  for any of the SAS in this study as this would have made comparison of their genotoxicity irrelevant. SAS cytotoxicity in V79 can be ranked as follows: Col 15 > Pyr 20 = Pre 20 > Pyr 25/70 = Col 40/80.

### Apoptosis

Pyr 20, Pre 20 and Col 15 all increased caspase-3 activity in V79. The increases were concentration dependent for Pyr 20 and Pre 20, but occurred only at the highest concentration for Col 15 (Figure 3). In contrast, no change in caspase activity was observed with Pyr 25/70 and Col 40/80. At a concentration of  $100 \text{ }\mu\text{g cm}^{-2}$ , Pyr 20, Pre 20 and Col 15 induced caspase activity increases of  $4.6 \pm 0.4$ ,  $2.6 \pm 0.8$  and  $8.1 \pm 2.5$ -fold, respectively, compared with the control. FBS deprivation for 18 h (positive control) was associated with a  $14.0 \pm 1.6$ -fold increase in caspase activity. The specificity of the caspase-3 assay was verified by extinction of the fluorescent signal in the presence of a peptide inhibitor in samples treated at  $100 \text{ }\mu\text{g cm}^{-2}$  SAS and in the positive control. Pyr 20 and Col 15 similarly increased the frequency of apoptotic cells, as observed in slides prepared for the micronucleus assays (additional graph, Figure 3). The effect of Pyr 20 was significant at two doses and the effect of Col 15 was significant at one dose. At

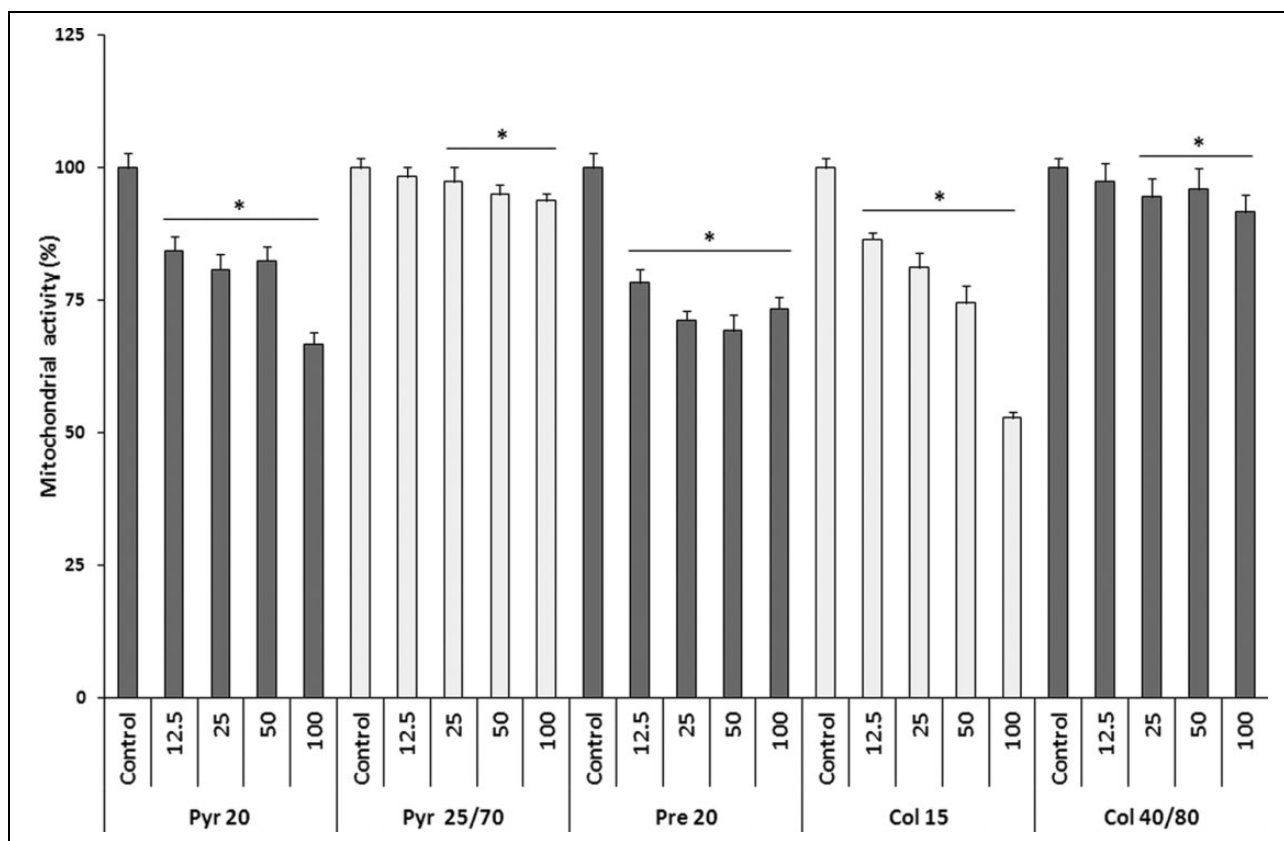


**Figure 2.** Percentage cell viability in V79 cells exposed to different concentrations of SAS ( $\mu\text{g cm}^{-2}$ ) over 24 h. Results are expressed as mean  $\pm$  SD. \* $p < 0.05$ : significantly different from the control. SAS: synthetic amorphous silica.

$100 \mu\text{g cm}^{-2}$ ,  $23 \pm 6$  apoptotic cells were observed in 1000 cells for Pyr 20 and  $83 \pm 20$  apoptotic cells were observed in 1000 cells for Col 15. These compare to  $1 \pm 2$  apoptotic cells for the control. The absence of apoptotic cell induction for Pyr 25/70 and Col 40/80 is consistent with the negative responses of these samples in the caspase-3 assay. In contrast, no increase in the number of apoptotic cells was detected for Pre 20 even though this SAS was positive in the caspase-3 assay. It is possible that caspase-3-positive cells induced by Pre 20 had not yet appeared as apoptotic cells at the time of the observation. As expected, FBS deprivation for 18 h significantly increased the frequency of apoptotic cells ( $86 \pm 11$  apoptotic cells among 1000 cells).

### DNA damage

No DNA damage was revealed by comet assays performed after 3 h of exposure to any of the SAS (data not shown). After 24 h of exposure, Pyr 20 and Col 15 were positive in comet assays performed both with and without FPG, whilst no DNA damage was

detected for Pyr 25/70, Pre 20 and Col 40/80 (Figure 4). Pyr 20 induced DNA-strand breaks at the highest concentration ( $100 \mu\text{g cm}^{-2}$ ) in assays performed without FPG and at all concentrations in the FPG-modified comet assays. A dose-dependent response was also observed for Col 15 in the FPG-modified comet assays (significant at 50 and  $100 \mu\text{g cm}^{-2}$ ) but only one concentration of Col 15 was positive ( $50 \mu\text{g cm}^{-2}$ ) in assays performed without FPG. Pyr 20 induced more DNA damage than Col 15 both with or without FPG. At  $100 \mu\text{g cm}^{-2}$ , the percentage of tail DNA in FPG assays was  $23.3 \pm 3.7\%$  for Pyr 20 and  $11 \pm 2\%$  for Col 15, compared with  $8.8 \pm 0.5$  and  $1.6 \pm 0.3\%$  for the respective controls. After 24 h treatment with the MMS-positive control ( $125 \mu\text{M}$ ), the mean percentages of tail DNA measured were  $5.9 \pm 2.7\%$  with FPG and  $70.1 \pm 5.5\%$  without FPG.

### Intracellular ROS, micronucleus formation and HPRT mutagenesis

No significant ROS induction, micronucleus formation or HPRT mutagenesis was detected in V79 cells

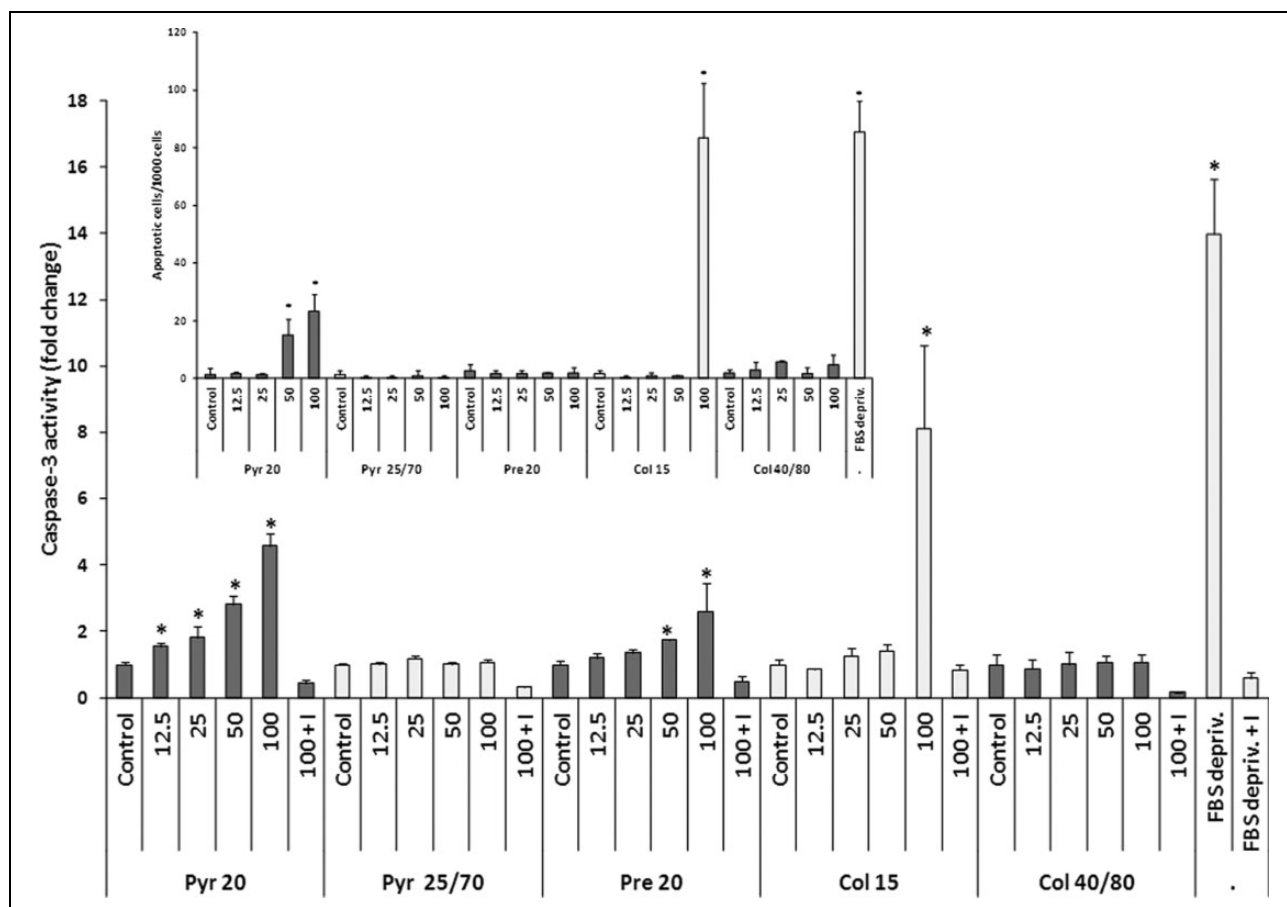


**Figure 3.** Apoptosis results: the main graph shows the induction of caspase-3 activity (fold change with respect to the control) in V79 cells exposed to different concentration of SAS ( $\mu\text{g cm}^{-2}$ ) over 24 h. At  $100 \mu\text{g cm}^{-2}$ , caspase-3 assays were performed both with and without the inhibitor (I) of the fluorescent substrate used in caspase-3 assays. The inset graph shows the frequency of apoptotic cells scored in 1000 V79 cells after to the same treatment. As positive control, V79 cells were cultured in FBS-free medium over 18 h. Results are expressed as mean  $\pm$  SD. \* $p < 0.05$ : significantly different from the control. SAS: synthetic amorphous silica; FBS: foetal bovine serum.

that had been exposed to SAS for 24 h. ROS assays performed with SAS were all negative (data not shown). The sensitivity of the ROS assay was verified using a  $\text{TiO}_2$  anatase sample that had previously been shown to increase intracellular ROS in DCFDA-based assays (Guichard et al., 2012). Micronucleus and HPRT results are shown in Table 2. In the micronucleus assays, MMS was used as a positive chemical control because of its known cytogenetic effect in V79 (Lasne et al., 1984). MMS (125  $\mu\text{M}$ ) induced significant micronuclei formation, with an average of  $100 \pm 21$  micronucleated cells per 1000 cells compared with an average of  $14 \pm 4$  micronucleated cells per 1000 cells in the control assays. HPRT assays were validated by using EMS as a positive control, as described by Davies et al. (1993). EMS (400  $\mu\text{M}$ ) caused a significant increase in the mutation

frequency (producing an average of  $110 \pm 20$  mutants per  $10^6$  cells compared with an average of  $27 \pm 3$  mutants per  $10^6$  cells in the control assays). No significant change in cloning efficiency was observed in cultures treated with SAS or with EMS at the time of HPRT mutation analysis (data not shown). The cloning efficiency was on average  $81 \pm 3\%$  for all cultures.

## Discussion

In this study, we evaluated the cytotoxic and genotoxic effects of five samples of different types of manufactured SAS on V79 Chinese hamster lung fibroblast. The choice of this pulmonary rodent cell line was primarily based on its suitability for use in cytogenetic assays according to OCDE guidelines.



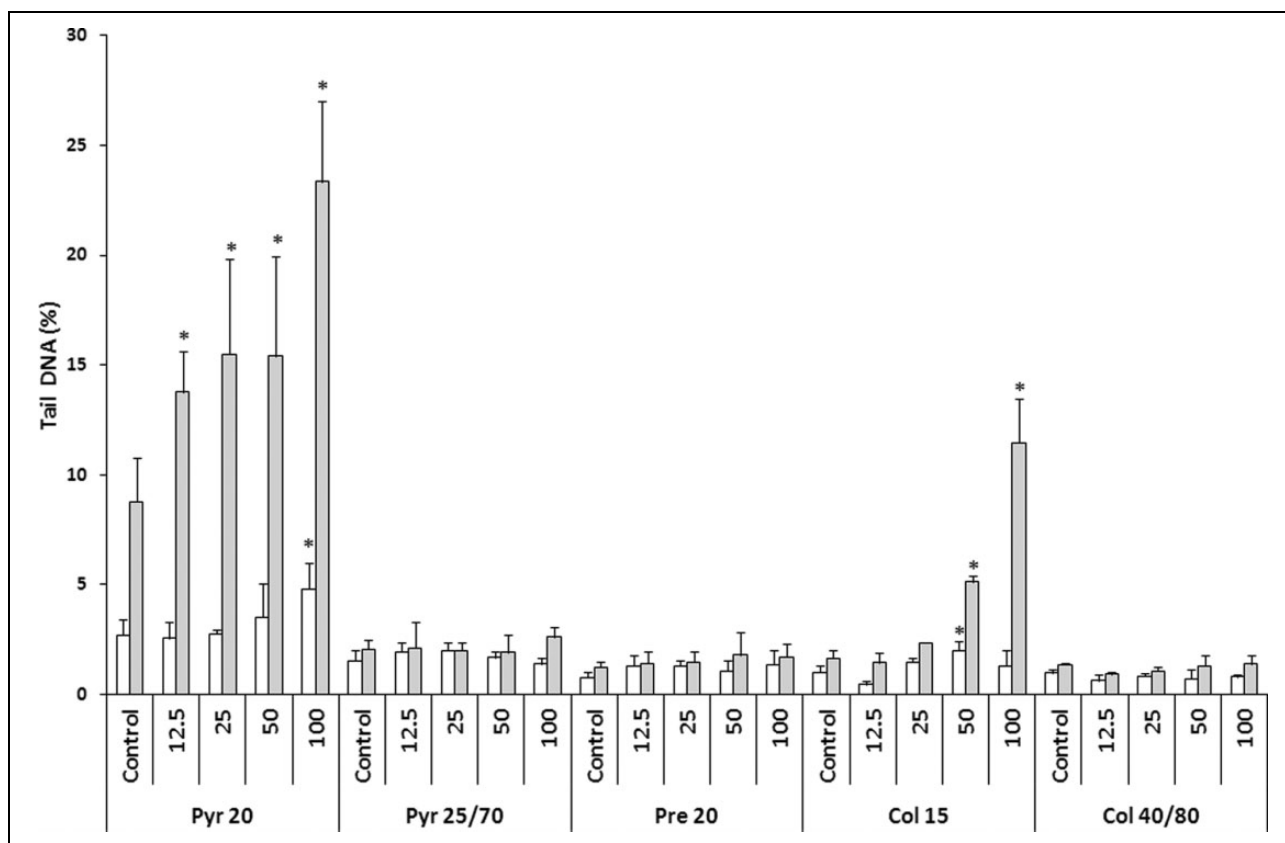


**Figure 4.** DNA damage expressed as the percentage of DNA in tail in V79 cells exposed for 24 h to either different concentrations of SAS ( $\mu\text{g cm}^{-2}$ ) or 125  $\mu\text{M}$  MMS (positive control). Comet assays were performed both without FPG (open histogram) and with FPG (filled histogram). Results are expressed as mean  $\pm$  SD. \* $p < 0.05$ : significantly different from the control. SAS: synthetic amorphous silica; FPG: formamidopyrimidine DNA glycosylase; MMS: methyl methanesulphonate.

In addition, our laboratory has previously demonstrated the ability of V79 cells to uptake particulate substances and the high sensitivity of these cells in HPRT assays (Elias et al., 1986). The selected SAS samples were obtained directly from industrial producers. The availability of pyrogenic and colloidal samples of different particle sizes provided an opportunity to compare size effects for these SAS.

SAS preparation for cell treatment was based on a standardized dispersion method that uses BSA as a dispersant. The principle of this method is to create protein coronas around SAS particles in order to stabilize particle suspensions and reduce particle agglomeration and sedimentation in the culture media (Jensen et al., 2011). This method was effective for almost all of the SAS used in this study, as agglomerate size was in the nanometric or submicrometric range in the culture medium. However, the technique proved less successful for the precipitated SAS sample (Pre 20) and agglomerates of several microns in size were still present after dispersion in BSA–water

or in the culture medium. When we compare the different SAS used in this study, there appears to be no obvious relationship between the sizes of agglomerates in culture medium and their cytotoxic effects. For example, the Col 40/80 sample formed the smallest aggregates but was not the most cytotoxic SAS in this study. Thus, physical properties other than aggregation/agglomeration are probably involved. For example, it has been suggested that the cytotoxic activity of SAS nanoparticles is influenced more by particle surface area than by the degree of agglomeration (Rabolli et al., 2011).

Under our culture and treatment conditions, only the SAS of smaller primary size (around 20 nm) clearly impaired cell viability. It is interesting to note that the minor difference in size between the finest-grained SAS (Pyr 20, Pre 20 and Col 15) and the coarser-grained SAS (Pyr 25/70 and Col 40/80) is associated with a significant difference in toxicity. Our results are consistent with the general consensus that the biological effect of particles increases

**Table 2.** Results of micronucleus and HPRT assays performed in V79 cells exposed to SAS for 24 h.

		Micronucleated cell frequency per 1000 cells <sup>a</sup>	HPRT mutant frequency per 10 <sup>6</sup> cells <sup>a</sup>
Pyr 20	Control	13.00 ± 4.36	27.30 ± 6.12
	12.5 µg cm <sup>-2</sup>	12.00 ± 1.73	44.29 ± 13.53
	25 µg cm <sup>-2</sup>	12.31 ± 7.21	21.24 ± 14.28
	50 µg cm <sup>-2</sup>	9.33 ± 0.58	22.78 ± 18.12
	100 µg cm <sup>-2</sup>	11.33 ± 6.03	23.06 ± 7.11
Pyr 25/70	Control	9.34 ± 1.52	30.74 ± 9.21
	12.5 µg cm <sup>-2</sup>	9.00 ± 5.57	37.34 ± 15.12
	25 µg cm <sup>-2</sup>	9.00 ± 2.65	18.03 ± 14.83
	50 µg cm <sup>-2</sup>	6.00 ± 1.00	17.72 ± 9.02
	100 µg cm <sup>-2</sup>	6.00 ± 2.00	22.60 ± 14.38
Pre 20	Control	11.67 ± 2.08	25.29 ± 22.74
	12.5 µg cm <sup>-2</sup>	7.67 ± 1.53	24.82 ± 16.67
	25 µg cm <sup>-2</sup>	7.33 ± 1.15	39.93 ± 10.29
	50 µg cm <sup>-2</sup>	9.67 ± 6.35	26.52 ± 4.41
	100 µg cm <sup>-2</sup>	12.34 ± 5.86	20.96 ± 3.13
Col 15	Control	14.66 ± 1.53	22.71 ± 13.81
	12.5 µg cm <sup>-2</sup>	12.90 ± 4.82	17.76 ± 12.22
	25 µg cm <sup>-2</sup>	14.65 ± 3.84	33.55 ± 24.63
	50 µg cm <sup>-2</sup>	14.61 ± 2.14	16.76 ± 16.45
	100 µg cm <sup>-2</sup>	12.67 ± 5.03	21.10 ± 18.10
Col 40/80	Control	19.00 ± 6.56	29.95 ± 26.17
	12.5 µg cm <sup>-2</sup>	20.33 ± 4.93	22.62 ± 12.49
	25 µg cm <sup>-2</sup>	22.67 ± 4.93	38.32 ± 24.94
	50 µg cm <sup>-2</sup>	15.33 ± 4.16	22.57 ± 14.38
	100 µg cm <sup>-2</sup>	18.66 ± 9.72	21.31 ± 16.44
Positive control <sup>b</sup>		75.00 ± 8.54 <sup>c</sup>	110.93 ± 19.58 <sup>c</sup>

HPRT: hypoxanthine guanine phosphoribosyltransferase; MMS: methyl methanesulphonate; EMS: ethyl methanesulphonate.

<sup>a</sup>Results are expressed as mean ± SD.

<sup>b</sup>The positive control was MMS (125 µM) in the micronucleus assay and EMS (400 µM) in the HPRT assay.

<sup>c</sup>*p* < 0.05: significantly different from the control.

inversely with size due to easier cellular uptake and/or to higher SSA, which greatly enhances surface reactivity (Oberdorster et al., 2005). The higher SSA values of Pyr 20, Pre 20 and Col 15 (≈200 m<sup>2</sup> g<sup>-1</sup>) compared with those of Pyr 25/75 and Col 40/80 (≈50 m<sup>2</sup> g<sup>-1</sup>) possibly reflect differential surface reactivity, which may in part explain the observed differences in their cytotoxicity and genotoxicity.

According our results, the effects of Pyr 20, Pre 20 and Col 15 on cell viability may involve apoptotic mechanisms and/or, in the case of Pyr 20 and Col 15, DNA damage. Recent *in vitro* studies have demonstrated the ability of different colloidal SAS to induce both apoptosis and DNA damage in

different lung and hepatic cell lines (Fede et al., 2012; Li et al., 2011; Ye et al., 2010). These effects were associated with increased intracellular ROS, lipid peroxidation and a decrease in glutathione content, indicative of cellular oxidative stress (Gerloff et al., 2009; Ye et al., 2010). In this study, the level of intracellular ROS remained unchanged in V79 cells treated with SAS. However, the enhanced responses of Pyr 20 and Col 15 in the presence of FPG in the comet assay can be considered indicative of oxidative DNA damage (Collins, 2004; Tice et al., 2000). The generation of DNA-strand breaks may be explained by indirect mechanisms involving intracellular ROS, but also by direct interactions between SAS particles and DNA, as has been suggested for other oxide nanoparticles (Brunner et al., 2006; Nel et al., 2006). However to our knowledge, no previous study of cellular uptake of SAS has reported the presence of particles in the nucleus, regardless of the particle size or cell line used (Drescher et al., 2011; Mu et al., 2012; Ye et al., 2010).

Our study showed no formation of micronuclei and no induction of HPRT mutation in V79 cells for all SAS. To our knowledge, no *in vitro* study of commercially available SAS has yet reported positive results in micronucleus assays or HPRT assays. Some studies showed a slight elevation in micronuclei frequency in A549 cells exposed to SAS synthesized for research purposes (Gonzalez et al., 2010, 2014). In addition, SAS of different sizes (30 and 80 nm) produced by the Stöber method were shown to induce gene mutation in 3T3-L1 mouse fibroblasts (Park et al., 2011). Although V79 cell line is known to be defective for the functional p53 protein, which is involved in DNA repair in response to DNA damage (Chaung et al., 1997), DNA damage induced by 24 h treatment with Pyr 20 and Col 15 did not lead to any chromosomal alteration or genomic mutation under our treatment conditions.

## Conclusions

Significant decreases in cell viability and an induction of apoptosis were observed in V79 cells exposed to pyrogenic and precipitated manufactured SAS of around 20 nm primary particle size. Pyrogenic and colloidal SAS of this size were also able to induce DNA damage. Pyrogenic and colloidal SAS of larger particle sizes (around 50 nm) yielded almost no toxicity in our experiments. None of the SAS samples generated micronuclei or HPRT mutations. Apoptosis

and DNA damage induced by pyrogenic and colloidal SAS of around 20 nm occurred without an elevation in intracellular ROS. However, as revealed in the FPG-modified comet assays, production of oxidative DNA lesions could not be excluded. In terms of hazard assessment, our study suggests that toxicity is related more to the primary particle size of the SAS than its type (pyrogenic or precipitated) or physical form (powder or colloid). Therefore, SAS materials of the same type but slightly different particle size (e.g. 20 and 25/70 nm) may possess very different cytotoxic and genotoxic properties. To gain a better understanding of the mechanisms that lead to DNA damage in V79 cells after SAS exposure, future studies could focus on alternative markers of oxidative stress such as lipid peroxidation and glutathione content. In addition, cellular TEM analysis would be useful for determining the outcome of SAS particles after their uptake by V79 cells, in particular, their intracellular location and their access to the cellular nucleus.

### Acknowledgments

The authors are grateful to Dr V. Matera (INRS) for ICP analyses and Mr O. Rastoix (INRS) for SEM analyses.

### Conflict of interest

The authors declared no conflicts of interest.

### Funding

This research received no specific grant from any funding agency in the public, commercial, or not-for-profit sectors.

### References

- Barnes CA, Elsaesser A, Arkusz J, et al. (2008) Reproducible comet assay of amorphous silica nanoparticles detects no genotoxicity. *Nano Letters* 8(9): 3069–3074.
- Brunauer S, Emmet PH and Teller E (1938) Adsorption of gases in multimolecular layers. *Journal of the American Chemical Society* 60: 309–319.
- Brunner TJ, Wick P, Manser P, et al. (2006) In vitro cytotoxicity of oxide nanoparticles: Comparison to asbestos, silica, and the effect of particle solubility. *Environmental Science and Technology* 40(14): 4374–4381.
- Chang W, Mi LJ and Boorstein RJ (1997) The p53 status of Chinese hamster V79 cells frequently used for studies on DNA damage and DNA repair. *Nucleic Acids Research* 25(5): 992–994.
- Collins AR (2004) The comet assay for DNA damage and repair: Principles, applications, and limitations. *Molecular Biotechnology* 26(3): 249–261.
- Collins AR, Gedik CM, Olmedilla B, et al. (1998) Oxidative DNA damage measured in human lymphocytes: Large differences between sexes and between countries, and correlations with heart disease mortality rates. *FASEB Journal* 12(13): 1397–1400.
- Davies MJ, Phillips BJ, Anderson D, et al. (1993) Molecular analysis of mutation at the hprt locus of Chinese hamster V79 cells induced by ethyl methanesulphonate and mitomycin C. *Mutation Research* 291(2): 117–124.
- Downs TR, Crosby ME, Hu T, et al. (2012) Silica nanoparticles administered at the maximum tolerated dose induce genotoxic effects through an inflammatory reaction while gold nanoparticles do not. *Mutation Research* 745(1–2): 38–50.
- Drescher D, Orts-Gil G, Laube G, et al. (2011) Toxicity of amorphous silica nanoparticles on eukaryotic cell model is determined by particle agglomeration and serum protein adsorption effects. *Analytical and Bioanalytical Chemistry* 400(5): 1367–1373.
- EC (2011) European Commission: Commission recommendation on the definition of nanomaterial. European Commission, Brussels, Belgium. Available at: <http://eur-lex.europa.eu/legal-content/> (accessed 6 February 2015).
- ECETOC (2006) Synthetic Amorphous Silica (Cas 7631-86-9). ECETOC JACC REPORT No. 51, 1–237.
- Elias Z, Poirot O, Schneider O, et al. (1986) Cellular uptake, cytotoxic and mutagenic effects of insoluble chromic oxide in V79 Chinese hamster cells. *Mutation Research* 169(3): 159–170.
- Fede C, Selvestrel F, Compagnin C, et al. (2012) The toxicity outcome of silica nanoparticles (Ludox(R)) is influenced by testing techniques and treatment modalities. *Analytical Bioanalytical Chemistry* 404(6–7): 1789–1802.
- Fruijtjer-Polloth C (2012) The toxicological mode of action and the safety of synthetic amorphous silica – A nanostructured material. *Toxicology* 294(2–3): 61–79.
- Gerloff K, Albrecht C, Boots AW, et al. (2009) Cytotoxicity and oxidative DNA damage by nanoparticles in human intestinal Caco-2 Cells. *Nanotoxicology* 3(4): 355–364.
- Gonzalez L, Lukamowicz-Rajska M, Thomassen LC, et al. (2014) Co-assessment of cell cycle and micronucleus frequencies demonstrates the influence of serum on the in vitro genotoxic response to amorphous monodisperse silica nanoparticles of varying sizes. *Nanotoxicology* 8(8): 876–884.
- Gonzalez L, Thomassen LC, Plas G, et al. (2010) Exploring the aneugenic and clastogenic potential in the nanosize range: A549 human lung carcinoma cells and amorphous monodisperse silica nanoparticles as models. *Nanotoxicology* 4: 382–395.

- Guichard Y, Schmit J, Darne C, et al. (2012) Cytotoxicity and genotoxicity of nanosized and microsized titanium dioxide and iron oxide particles in Syrian hamster embryo cells. *Annals of Occupational Hygiene* 56(5): 631–644.
- Hasan NM, Adams GE and Joiner MC (1999) Effect of serum starvation on expression and phosphorylation of PKC- $\alpha$  and p53 in V79 cells: Implications for cell death. *International Journal of Cancer* 80(3): 400–405.
- IARC (1997) Silica, some silicates, coal dust and para-Aramid fibrils. *International Agency for Research on Cancer – Monographs on the Evaluation of Carcinogenic Risks to Humans* 68: 1–506.
- Jensen KA, Kembouche Y, Christiansen E, et al. (2011) The generic NANOGENOTOX dispersion protocol – standard operation procedure (SOP). *NANOGENOTOX Deliverable Report No. 3*, June 2011. Available at: [http://www.nanogenotox.eu/files/PDF/Deliverables/nanogenotox\\_deliverable\\_wp5.pdf](http://www.nanogenotox.eu/files/PDF/Deliverables/nanogenotox_deliverable_wp5.pdf) (accessed 6 February 2015).
- Johnston CJ, Driscoll KE, Finkelstein JN, et al. (2000) Pulmonary chemokine and mutagenic responses in rats after subchronic inhalation of amorphous and crystalline silica. *Toxicological Sciences* 56(2): 405–413.
- Lasne C, Gu ZW, Venegas W, et al. (1984) The in vitro micronucleus assay for detection of cytogenetic effects induced by mutagen-carcinogens: Comparison with the in vitro sister-chromatid exchange assay. *Mutation Research* 130(4): 273–282.
- LeBel CP, Ischiropoulos H and Bondy SC (1992) Evaluation of the probe 2',7'-dichlorofluorescein as an indicator of reactive oxygen species formation and oxidative stress. *Chemical Research in Toxicology* 5(2): 227–231.
- Li Y, Sun L, Jin M, et al. (2011) Size-dependent cytotoxicity of amorphous silica nanoparticles in human hepatoma HepG2 cells. *Toxicology In Vitro* 25(7): 1343–1352.
- Mu Q, Hondow NS, Krzeminski L, et al. (2012) Mechanism of cellular uptake of genotoxic silica nanoparticles. *Particle and Fibre Toxicology* 9: 29.
- Napierska D, Thomassen LC, Lison D, et al. (2010) The nanosilica hazard: Another variable entity. *Particle and Fibre Toxicology* 7(1): 39.
- Nel A, Xia T, Madler L, et al. (2006) Toxic potential of materials at the nanolevel. *Science* 311(5761): 622–627.
- Oberdorster G, Oberdorster E and Oberdorster J (2005) Nanotoxicology: An emerging discipline evolving from studies of ultrafine particles. *Environmental Health Perspectives* 113(7): 823–839.
- Park MV, Verharen HW, Zwart E, et al. (2011) Genotoxicity evaluation of amorphous silica nanoparticles of different sizes using the micronucleus and the plasmid lacZ gene mutation assay. *Nanotoxicology* 5(2): 168–181.
- Rabolli V, Thomassen LC, Uwambayinema F, et al. (2011) The cytotoxic activity of amorphous silica nanoparticles is mainly influenced by surface area and not by aggregation. *Toxicology Letters* 206(2): 197–203.
- Speit G, Schutz P, Bonzheim I, et al. (2004) Sensitivity of the FPG protein towards alkylation damage in the comet assay. *Toxicology Letters* 146(2): 151–158.
- Tavares AM, Louro H, Antunes S, et al. (2014) Genotoxicity evaluation of nanosized titanium dioxide, synthetic amorphous silica and multi-walled carbon nanotubes in human lymphocytes. *Toxicology In Vitro* 28(1): 60–69.
- Tice RR, Agurell E, Anderson D, et al. (2000) Single cell gel/comet assay: Guidelines for in vitro and in vivo genetic toxicology testing. *Environmental and Molecular Mutagenesis* 35(3): 206–221.
- Ye Y, Liu J, Xu J, et al. (2010) Nano-SiO<sub>2</sub> induces apoptosis via activation of p53 and Bax mediated by oxidative stress in human hepatic cell line. *Toxicology In Vitro* 24(3): 751–758.